Frontiers of Information Technology & Electronic Engineering
www.jzus.zju.edu.cn; engineering.cae.cn; www.springerlink.com
ISSN 2095-9184 (print); ISSN 2095-9230 (online)
E-mail: jzus@zju.edu.cn

# Recognition of walking environments and gait period by surface electromyography*

Seulki KYEONG, Wonseok SHIN, Minjin YANG, Ung HEO, Ji-rou FENG, Jung KIM†‡

*Department of Mechanical Engineering, Korea Advanced Institute of Science and Technology (KAIST), Daejeon 34141, Korea*

†E-mail: jungkim@kaist.ac.kr

Received Sept. 27, 2018; Revision accepted Feb. 22, 2019; Crosschecked Mar. 14, 2019

**Abstract:** Recognizing and predicting the movement and intention of the wearer in control of an exoskeleton robot is very challenging. It is difficult for exoskeleton robots, which measure and drive human movements, to interact with humans. Therefore, many different types of sensors are needed. When using various sensors, a data design is needed for effective sensing. An electromyographic (EMG) signal can be used to identify intended motion before the actual movement, and the delay time can be shortened via control of the exoskeleton robot. Before using a lower limb exoskeleton to help in walking, the aim of this work is to distinguish the walking environment and gait period using various sensors, including the surface electromyography (sEMG) sensor. For this purpose, a gait experiment was performed on four subjects using the ground reaction force, human–robot interaction force, and position sensors with sEMG sensors. The purpose of this paper is to show progress with the use of sEMG when recognizing walking environments and the gait period with other sensors. For effective data design, we used a combination of sensor types, sEMG sensor locations, and sEMG features. The results obtained using an individual mechanical sensor together with sEMG showed improvement compared to the case of using an individual sensor, and the combination of sEMG and position information showed the best performance in the same number of combinations of three sensors. When four sensor combinations were used, the environment classification accuracy was 96.1%, and the gait period classification accuracy was 97.8%. Vastus medialis (VM) and gastrocnemius (GAS) were the most effective combinations of two muscle types among the five sEMG sensor locations on the legs, and the results were 74.4% in pre-heel contact (preHC) and 71.7% in pre-toe-off (preTO) for environment classification, and 68.0% for gait period classification, when using only the sEMG sensor. The two effective sEMG feature combinations were "mean absolute value (MAV), zero crossings (ZC)" and "MAV, waveform length (WL)", and the "MAV, ZC" results were 80.0%, 77.1%, and 75.5%. These results suggest that the sEMG signal can be effectively used to control an exoskeleton robot.

**Key words:** Walking environment; Gait Period; Surface electromyography (sEMG); Exoskeleton
https://doi.org/10.1631/FITEE.1800601 **CLC number:** TP242

## 1 Introduction

The need for assistive technology to help patients and workers handle heavy loads in activities where lower extremities are involved is continually increasing. Patients with neurological injuries, such as with a stroke or spinal cord injury, may have muscle weakness and movement disorders, which result in a lack of power in lower extremities when trying to move. Additionally, workers dealing with heavy loads, such as soldiers or heavy industry workers, need to supplement their muscular strength since they are frequently exposed to continuous working conditions involving heavy loads. Therefore, research on developing lower extremity exoskeletons to enhance muscular strength for medical, industrial, and military applications has been actively pursued (Colombo et al., 2000; Guizzo and Goldstein, 2005; Zoss et al., 2006; Veneman et al., 2007; Walsh et al., 2007; Sankai, 2010; Strausser and Kazerooni, 2011;

‡ Corresponding author
* Project supported by the Agency for Defense Development and Defense Acquisition Program Administration (No. UD160059BD)
ORCID: Jung KIM, https://orcid.org/0000-0002-1825-6325

Esquenazi et al., 2012; Sanz-Merodio et al., 2014).

The key technology in an exoskeleton is the ability to recognize human intention and effectively control the movement of the exoskeleton based on the perceived human intention (Yan et al., 2015). This comes about due to direct physical contact between the human and the exoskeleton. Failure to recognize human intention may lead to discomfort for the wearer because the exoskeleton may not help the person move as intended. Additionally, if a physical contact exoskeleton cannot be effectively controlled, the wearer may not only be inconvenienced, but a dangerous situation may even occur. Therefore, many exoskeleton studies have focused on human–robot interaction so that the exoskeleton can recognize human intention and exert robust control.

One of the frequently used methods for recognizing intention during locomotion is gait cycle classification (Walsh et al., 2007; Lewis and Ferris, 2011; Sasaki et al., 2013). A gait cycle is the cycle of the positions of the human leg, such as initiation and termination of the swing and stance phases, during level surface walking (Jung et al., 2015). This may vary from person to person and due to changes in the environment, but it gives a general distribution of the leg position over time, which can be used to predict when the next movement will take place and which muscles are contracted at a specific time. In other words, the gait cycle can be used to recognize the detailed intentions of leg movements during locomotion, which is an unconscious movement (Varol et al., 2010; Goršič et al., 2014; Jung et al., 2015).

Compared with gait cycle classification, there are few studies concerned with recognizing the walking environment. However, it is crucial that the walking environment be taken into account because system dynamics and kinematics change for different walking environments (Lawson et al., 2013). Pre-defined motions and controls to aid walking on a level surface cannot accurately aid when walking in different environments, such as on slopes and stairs, since the intention recognition strategy would change in the different environments (Young et al., 2013). Therefore, an algorithm that can recognize diverse environments would help enhance muscle strength more effectively and with more stability (Du et al., 2012). In addition to recognizing each type of walking environment, transitions between environments are also important. If the recognition and transition are performed accurately and quickly, the exoskeleton could more effectively provide assistance, even in uneven and complicated environments (Young and Ferris, 2017). Therefore, environment recognition is just as important.

Healthy people can naturally locomote and adjust their behavior in different walking environments without cognitive effort; however, given the complexity of human motor behavior, it is difficult for any type of robot including an exoskeleton to initiate even simple commensurate actions (Dotov et al., 2016; Gupta and Agarwal, 2018). In real situations, recognition of walking environments or locomotion modes and the preceding corresponding movements is essential for control of a robotic exoskeleton to complete tasks. Moreover, it is necessary to identify the different environments as soon as possible when the foot contacts the ground, in order to achieve stable and natural walking with the exoskeleton (Long et al., 2016; Kim et al., 2017a, 2017b).

Previous studies have used mechanical sensors and bio-signal sensors to recognize each environment (Jin et al., 2006; Zhang et al., 2011; Farrell, 2013; Martinez-Hernandez et al., 2018). A mechanical sensor, such as a ground reaction force (GRF) sensor or an inertial measurement unit (IMU) sensor, measures the human and robot kinematics and kinetic data. A mechanical sensor can be effective and thus has advantages, but the data are collected after the actual human movement is initiated, which results in a time delay. Therefore, external resistance precedes the exoskeleton movement, which the wearer needs to overcome. A surface electromyography (sEMG) sensor is a non-invasive bio-signal sensor that measures how much a certain muscle is activated. Since it can detect the activation of muscle, it may be used in an exoskeleton for intention recognition (Lenzi et al., 2013). These bio-signal sensors, such as the sEMG sensor, can collect signals prior to human movement, which means it can predict motion (Lenzi et al., 2012). However, it has a disadvantage in that its signal is rather noisy and the signal may vary due to muscle fatigue and changes in the area on the skin where it is attached (Cifrek et al., 2009).

An EMG signal is used in two ways in exoskeleton research. First, it is used to verify the effects of the control methods (Kim et al., 2017b). Most

exoskeleton studies demonstrate the performance of their exoskeletons or control algorithms through decreasing EMG activities or metabolic cost. Second, the EMG signal is used as a control input of the exoskeleton. EMG-based control studies estimate torque, velocity, stiffness (Kawamoto et al., 2003) or verify their states (Huang et al., 2009; Young and Ferris, 2017).

The aim of this study is to recognize and predict the walking environment and gait period. We classify walking environments and gait periods using data from various sensors. To determine the appropriate conditions, we use a combination of various sensors, sEMG features, and sEMG attachment locations. Using these predictions, exoskeleton control can be performed under various circumstances based on gait periods.

## 2 Methods

### 2.1 Experimental setup

Walking experiments were conducted with the lower limb sensing suit system, which is discussed in Section 2.2. The upper body in the lower limb sensing suit system is outfitted with a setup box containing a processor, data acquisition systems, battery, and other sensing systems. To measure the gait motion, we used a minicomputer as a processor, and sensing data were acquired using the Simulink software in MATLAB 2016b (The MathWorks, Inc., USA) and QUARC 2.6 (Quanser, Canada). We used two data acquisition boards, NI USB-6211 and NI USB-6251 (National Instruments Inc., USA).

Four subjects (age, 24.4±3.0 years old; height, 172.8±5.0 cm; weight, 73.2±3.6 kg) participated in the experiments covering five different walking environments: level walking, ramp ascent/descent, and stair ascent/descent.

The experiment was conducted with 10 sets, each set comprising a hybrid terrain involving level walking, ramp ascent, level walking, stair descent, level walking, stair ascent, level walking, ramp descent, and level walking. The total length for level walking was 18.5 m, the angle of the ramp was 10° (Young et al., 2014), and the width and height of the stairs were 60 and 10 cm, respectively. For classification of the walking environment, various walking environment experiment sets were analyzed, and for classification of the gait period, only the level walking section was analyzed.

### 2.2 Lower limb sensing suit system

We developed a sensing suit for lower limb motion detection. The system has three-degree-of-freedom (3-DOF) motion in each leg at the hip, knee, and ankle joints with frictionless components to measure multiple types of motion. There were no mechanical structures that limit the range of motion in each joint; instead of using actuator units which would hinder the subjects' natural motion, the system simply used ball bearings for axial direction constraints. Additionally, in the connecting parts of the carbon frame there was an aluminum case structure for aligning carbon column with the thigh and calf length and axis. This part reduces the slip and overcompression between the suit and the human at each junction of the braces for the human.

Fig. 1a shows the experimenter wearing the sensing suit system. The lower limb sensing suit system consists of a body frame with the following mechanical and bio sensors: position sensors, GRF sensors, interaction force sensors, and sEMG sensors.

We used a magnetic type optical encoder as the position sensor to measure the rotary angle of the hip, knee, and ankle joints.

The GRF sensors measured the GRFs at the four major parts of the foot. Fig. 2a shows the four major parts of the foot including the toe, meta 12, meta 45, and the heel (Kong and Tomizuka, 2009). The GRF sensing system consisted of a sensor embedded foot plate, which captured data from heel contact to toe off. The system we used was an insole type with four integrated sensors. The sensors were located in the toe,

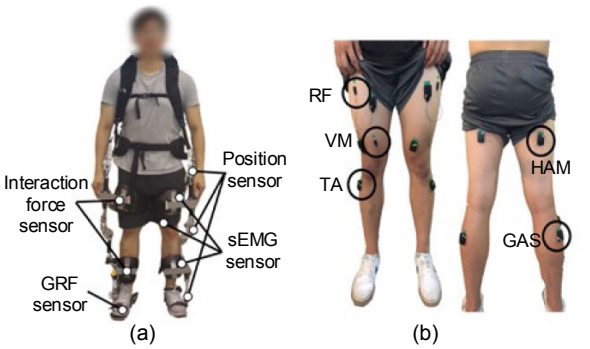


**Fig. 1 Experimental setup: (a) lower limb sensing suit system; (b) attachment positions of the sEMG sensors**
RF: rectus femoris; VM: vastus medialis; TA: tibialis anterior; HAM: hamstring; GAS: gastrocnemius

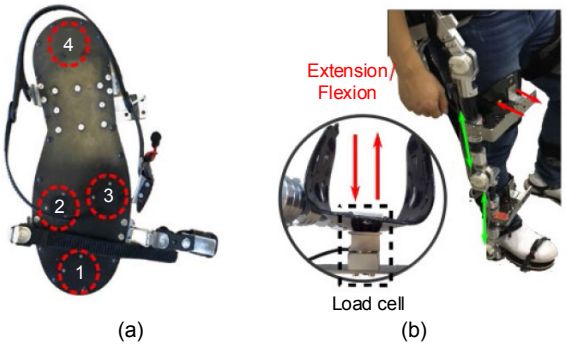


**Fig. 2 GRF sensor embedded foot plate (a) and interaction force sensing structure (b)**
In (a), 1, 2, 3, and 4 represent the toe, meta 12, meta 45, and the heel, respectively

meta 12, meta 45, and the heel. The correlation between each sensing module was minimized, and the footplate size was fitted for a normal-size adult.

The human–robot interaction force estimation was executed with a single-ended structure, which was fixed to the robot body frame. Fig. 2b shows the interaction force sensing structure. Human intention can also be detected using the interaction force module, consisting of a load cell that was embedded in a knee brace. A fixed single-ended plate was used to measure the relative extents of compression and extension in the load cell. A positive sign in the load cell implied human joint flexion, and a negative sign implied extension of the lower limb joint. The brace was fixed to the human body using a Velcro-type strap that surrounded the thigh or calf. The height of the Velcro strap was different for the users and we adjusted it using a varying-link-length structure.

The sEMG sensors were attached to five leg muscles: vastus medialis (VM), hamstring (HAM), tibialis anterior (TA), gastrocnemius (GAS), and rectus femoris (RF). The sEMG sensors took measurements at 2 kHz using the Trigno system (Delsys, USA). Fig. 1b shows the attachment positions of the sEMG sensors. All data were processed with a bandpass filter of 20 to 500 Hz and a band-stop filter of 59 to 61 Hz.

## 2.3 Signal processing of sEMG and mechanical sensors

### 2.3.1 Walking environment classifications

In the case of environment classification, another experimenter classified the environment using an analog switch to distinguish it from the reference environment. The change in the environment was based on the beginning of the heel contact of the foot.

To identify the walking environments and compare the performance of different combinations of sensors, a high performance and effective classifier was needed to obtain reliable results. In previous studies on sEMG pattern recognition based control of prostheses, classification performance comparison has been reported among different types of classifiers for locomotion mode identification (Huang et al., 2009, 2011). A pattern classification algorithm is required to identify the walking environment and gait period. Of the various pattern classification algorithms, Bayesian linear discriminant analysis (BLDA) was chosen. BLDA is simple and a typical representative of statistical classifiers using non-recursive training to produce linear boundaries. This classifier has been widely used in EMG pattern classification as its computational efficiency and classification performance are comparable to the counterparts of other classification algorithms (Huang et al., 2011). In previous research, the classification performances of BLDA and a more complex artificial neural network (ANN) classifier have been compared. For sEMG, from all the studied phases (PreHC, PostHC, PreTO, PostTO) in Huang et al. (2011), BLDA showed lower classification errors. For sEMG, from the whole stride cycle without divided phases, although a significantly higher error can be observed, the BLDA method still showed lower classification errors compared with the ANN classifier. Since parameter regularization must be considered when using a complex ANN classifier, we determined that, in terms of classification accuracy, degree of facility, and computational efficiency, the BLDA classifier was the first choice for our study.

The stride cycle is determined by the GRF sensor. We collected the four parts of the GRF data and summed the four kinds of data for stride separation. Based on the heel-contact and toe-off points obtained from the GRF signals, all data sets were extracted for two cases per 200 ms before the heel-contact (preHC) and toe-off (preTO) (Huang et al., 2009). Fig. 3 shows preHC and preTO during the gait on a timeline. The preHC is related to the terminal swing period and the start of the swing phase. The preTO relates to the pre-swing period and the start of the swing phase (Neumann, 2002). We used these data sets to classify the walking environment discussed in Section 3.1.

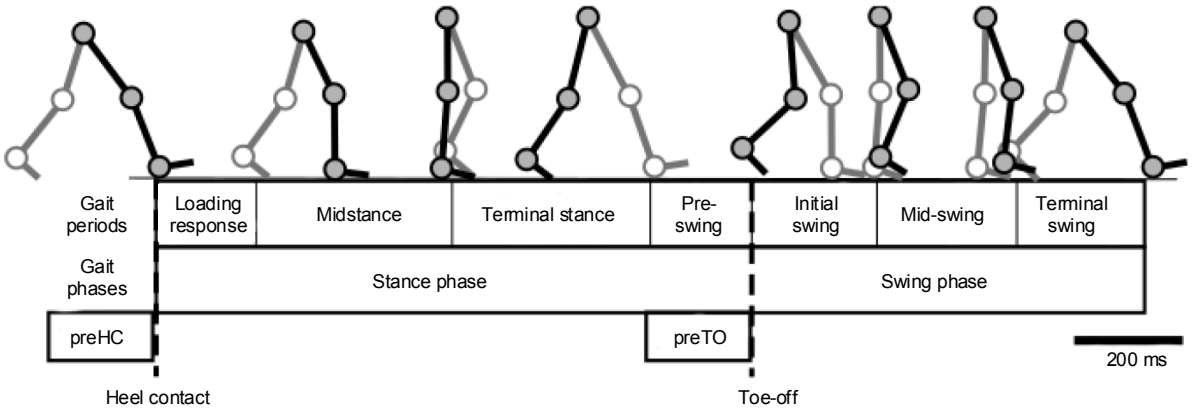


**Fig. 3 Gait period and gait sections of preHC and preTO**

We used four kinds of features in one data set. The GRF feature consists of information about the four positions in the foot for four time periods. The position feature consists of information about three joint angles for four time periods. The interaction force feature consists of information about two points in the link for four time periods, and the sEMG feature consists of information about five locations on the leg for four kinds of sEMG features.

For each case, the signals of the four parts of the GRF were divided into four sections of 50 ms for 200 ms before the heel-contact and toe-off, and the average value of each part was used as the GRF feature. A GRF feature vector of size 16 was obtained for each gait section.

Similar to GRF sensors, the feature value of the position sensor was used as the average value for 50 ms divided by a quarter of the corresponding 200 ms. The three joint angles of the legs were measured, and four features were extracted for each joint angle. A position feature vector of size 12 was obtained for each gait section.

Like GRF and position sensors, the feature values of the interaction force sensor were made up of average values from each sensor four times in 50 ms increments. For the two points on the thigh and calf links, the interaction force between the experimenter and the sensing suit system was measured, and the feature was calculated. An interaction force feature vector of size eight was obtained for each gait section.

For sEMG signals, we used the four time- and frequency-domain features, mean absolute value (MAV), zero crossings (ZC), slope sign changes (SSC), and waveform length (WL). The four methods for obtaining sEMG features are defined below:

$$\mathrm{MAV}_i = \frac{1}{N}\sum_{k=1}^{N} |x_i(k)|, \tag{1}$$

$$\mathrm{ZC}_i = \sum_{k=2}^{N-1} f(k), \tag{2}$$

where

$$f(x) = \begin{cases} 1, & x_i(k)x_i(k+1) < 0 \text{ and} \\ & |x_i(k) - x_i(k+1)| \geq \varepsilon, \\ 0, & \text{otherwise,} \end{cases}$$

$$\mathrm{SSC}_i = \sum_{k=2}^{N-1} f[(x_i(k) - x_i(k-1))(x_i(k) - x_i(k+1))], \tag{3}$$

where

$$f(x) = \begin{cases} 1, & x \geq \varepsilon, \\ 0, & \text{otherwise,} \end{cases}$$

$$\mathrm{WL}_i = \sum_{k=1}^{N-1} |x_i(k) - x_i(k+1)|. \tag{4}$$

These features were chosen because they enable a simpler and faster computation compared to the frequency-domain features while still providing information about the signal's frequencies through ZC and SSC. As shown in Fig. 3, the features were extracted from the sEMG signals just before the heel contacted the ground and the toe lifted off the ground, a moment determined by the GRF readings for a duration of 200 ms. Because we measured five different muscles and extracted four features for each muscle sEMG signal, a feature vector of size 20 was obtained for each gait section. For each section of the gait, leave-one-out cross-validation was used to train and test the accuracy of the BLDA classifier.

2.3.2 Gait period classifications

The seven gait periods proposed by Perry and Davids (1992) (loading response, mid-stance, terminal stance, pre-swing, initial swing, mid-swing, and terminal swing) were distinguished by eight gait events (initial contact, opposite toe off, heel rise, opposite initial contact, toe off, feet adjacent, tibia vertical, and next initial contact). Fig. 3 shows the gait periods and gait phases determined by gait events. We detected six gait periods with integrated mid-swing and terminal swing periods, based on the heel-contact, heel-off, and toe-off points using the GRF of both feet. We classified the mid-swing and the terminal swing based on the point where the GRF sum was at a maximum.

In the case of gait period classification, one feature set consisted of the average value of the interval. This is because the duration of each gait period is different. The configuration of the feature set is the same as that in environment classification, and in the case of features that averaged 50 ms, the values were integrated.

## 3 Discussion and results

### 3.1 Walking environments classification

3.1.1 Combination of sEMG, GRF, position, and interaction force sensors

To classify the five kinds of walking environments, level-ground walking, stair ascent/descent, and ramp ascent/descent, an environment classification was performed using different combinations of sensors to find the effective combinations according to the sensors. Fig. 4 and Table 1 show the error values for the accuracy of the classification of the walking environment according to the sensor combinations. The $x$ axis was divided into dotted lines according to the two time periods, preHC and preTO. For each time period, we classified the walking environment based on different sensor combinations. The classification performance was poor when using a single sensor except for the position sensor. However, when the bio-signals and mechanical signals of "sEMG, position sensors," "sEMG, GRF sensors," or "sEMG, interaction force sensors" were used together, the classification error was reduced by 10%. When using sEMG together with individual sensors, the performance quality was better than when using individual sensors only. The GRF decreased by 7.3% in preHC and by 10.5% in preTO, and the interaction force decreased by 9.3% in preHC and by 6.9% in preTO. The second through fifth rows from the back in Table 1 show the results of using three sensor combinations. The combination included the sEMG sensor and position sensor that had the highest

**Table 1 Walking environment classification results according to the sensor combinations for the pre-heel contact condition**

| Sensor combination | Classification accuracy (%) |
|---|---|
| EMG | 76.7±2.5 |
| GRF | 79.4±16.0 |
| Position | 93.3±9.2 |
| IntF | 79.5±2.7 |
| EMG, GRF | 86.7±9.6 |
| EMG, Position | 94.1±6.6 |
| EMG, IntF | 88.8±4.2 |
| EMG, GRF, Position | 95.8±6.3 |
| EMG, GRF, IntF | 88.9±7.6 |
| EMG, Position, IntF | 96.0±4.1 |
| GRF, Position, IntF | 95.4±6.7 |
| EMG, GRF, IntF, Position | 96.1±4.6 |

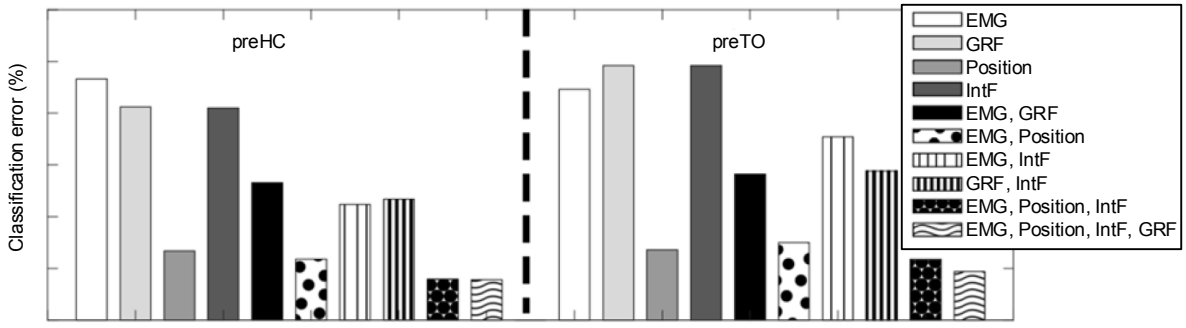


**Fig. 4 Walking environment classification errors after combining the sensor data for the sEMG, GRF, position, and interaction forces for different gait periods**

classification accuracy. When sEMG and position information was combined in the same number of combinations, the classification quality was increased. In the case of using the four sensors together, the error was similar to that in the case using "sEMG, position, interaction forces sensors," and the error was 3.9% for preHC and 4.7% for preTO. In the case of the preHC condition, this means that the stance phase can be predicted by classifying the walking environment before reaching the heel. Additionally, in the case of the preTO condition, this means that the swing phase can be predicted by classifying the environment before the toe leaves the ground.

Table 2 shows the confusion matrix of the walking environment classification for subject 03 using sEMG, position, and interaction force sensors. In level walking, only 0.3% was misclassified as stair ascent. Stair ascent was 100% correctly classified. For ramp ascent, 86.4% was correctly classified, and the remaining 13.6% was classified as stair ascent. Ramp descent was 94.7% correctly classified, and the remaining 5.3% was classified as stair descent. In stair descent, 85.0% was correctly classified, and the remaining 15.0% was classified as ramp ascent. In the cases of misclassification, most misclassified ascent environments were classified as the other type of ascent, while misclassified descent environments were classified as the other type of descent. In the case of the other subjects, most of the misclassified cases were similar in the ascending and descending environments. It was concluded that the movement is similar to the ascending and descending movements. Other misclassified cases revealed with the other subjects were the stair descent case. In this case, an average of 2.4% was misclassified as level walking.

**Table 2 Confusion matrix for the classification of the five walking environments using sEMG, position, and interaction force sensors by BLDA (%)**

| Walking environment | Level walking | Ramp ascent | Ramp descent | Stair ascent | Stair descent |
|---|---|---|---|---|---|
| Level walking | 99.0 | 0.7 | 0.0 | 0.3 | 0.0 |
| Ramp ascent | 0.0 | 86.4 | 0.0 | 13.6 | 0.0 |
| Ramp descent | 0.0 | 0.0 | 94.7 | 0.0 | 5.3 |
| Stair ascent | 0.0 | 0.0 | 0.0 | 100.0 | 0.0 |
| Stair descent | 0.0 | 0.0 | 15.0 | 0.0 | 85.0 |

Huang' 2009 study of eight subjects using sEMG alone had a classification error of 5.2% for the preHC condition, and 6.0% for the preTO condition (Huang et al., 2009). Young's 2014 study of eight amputee subjects using sEMG and mechanical sensor data had classification errors of 3.8% to 1.0% (Young et al., 2014). Because the location and number of sensors are different in our study, and previous studies were for amputees using prostheses, it is difficult to compare the results accurately, but the classification results are still similar to those in previous studies.

### 3.1.2 Combination of sEMG sensor locations

In this experiment, the sEMG sensors were attached to the legs with five sEMG sensors per leg, and the signals from a total of 10 sEMG sensors were measured. In this classification, we performed an experiment to determine the optimal sEMG sensor combination for classifying the walking environment. The types of combinations were as follows: a case in which all the sensors were integrated, a case in which four sensors for the four muscle positions around the knee were used, and a case in which a combination of the two sensors was used.

Table 3 shows the results of the classification including the other sensors (GRF, position, and interaction force sensors), and the combination of the sEMG sensors by subjects. This result corresponds to the preHC case, and the trend for the preTO case was not significantly different. The effect of the other sensors was large compared to the change in the sEMG sensor combination, and the results did not significantly change. The standard deviation value was not large depending on the combination. Therefore, in Table 4 the influence of sensors other than the sEMG sensors was excluded.

**Table 3 Walking environment classification results according to the sEMG sensor location combinations with other sensors for preHC**

| Sensor location | Classification accuracy (%) | | | |
|---|---|---|---|---|
| | S01 | S02 | S03 | S04 |
| All locations | 99.9 | 98.2 | 97.0 | 89.4 |
| VM, HAM, TA, GAS | 99.9 | 97.5 | 96.9 | 90.5 |
| VM, TA | 99.9 | 96.7 | 97.0 | 89.6 |
| VM, GAS | 99.0 | 97.5 | 96.9 | 84.0 |
| HAM, GAS | 99.9 | 98.3 | 96.0 | 89.7 |
| TA, GAS | 99.9 | 98.3 | 97.0 | 92.3 |
| Average | 99.8 ±0.4 | 97.7 ±0.6 | 96.8 ±0.4 | 89.2 ±2.8 |

**Table 4 Walking environment classification results according to the sEMG sensor location combinations without other sensors for preHC and preTO**

| Sensor combination | Classification accuracy (%) | |
|---|---|---|
| | preHC | preTO |
| All locations | 76.7±2.5 | 77.7±11.6 |
| VM, HAM, TA, GAS | 75.0±1.0 | 77.1±8.1 |
| VM, TA | 66.9±6.7 | 73.9±8.2 |
| VM, GAS | 74.4±3.8 | 71.7±14.3 |
| HAM, GAS | 66.7±7.6 | 63.5±10.7 |
| TA, GAS | 50.2±10.7 | 52.1±7.0 |

Table 4 shows the results obtained for classification using only sEMG sensors. The performance when using all the sensors was the highest, but it was similar to the performance when using only sensors for the four muscles around the knee. The reason for analyzing the combination of the four muscles around the knee was to confirm the ease of wearing the sensors for the development of a future sEMG suit. Additionally, when two sensors were combined, the combination of VM and GAS was the most accurate for the preHC case, and the combination of VM and TA was the most accurate for the preTO case. It was concluded that, when not using all five sensors, similar results can be obtained when measuring the sEMG location of the VM and GAS or VM and TA muscle positions.

3.1.3 Combination of sEMG sensor features

There are several types of sEMG features, including MAV, ZC, SSC, and WL. We compared the combinations of MAV, ZC, SSC, and WL to determine which features were effective. In Table 3, when the other sensors and the combination of the sEMG sensors were compared, there was no significant difference. Therefore, only the feature combinations of the sEMG sensors were used and we did not include other sensors' information. In this case, the position of the sEMG sensor included all five positions. Fig. 5 shows the results of classifying the walking environment by changing the combinations of sEMG features. "MAV, ZC" or "MAV, WL" combinations were the most accurate compared to using all four features for the preHC case. For the preTO case, the classification accuracy of these combinations was not the highest, but the results were similar to those in the case of using all four features, which is a combination of the time- and frequency-domain features.

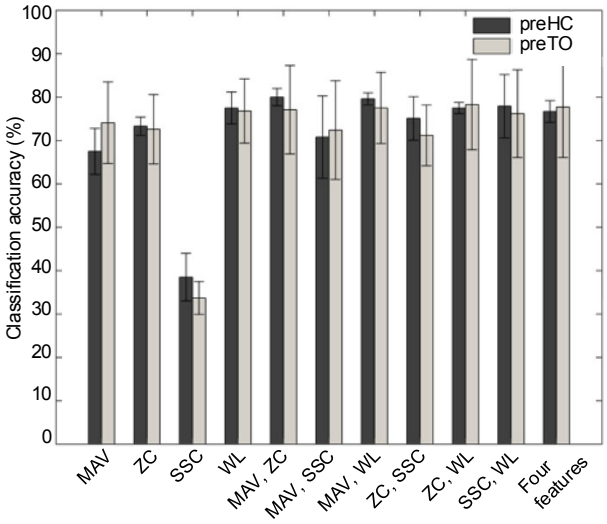


**Fig. 5 Walking environment classification results according to the sEMG feature combinations without other sensors for preHC and preTO**

## 3.2 Gait period classifications

3.2.1 Combination of sEMG, GRF, position, and interaction force sensors

Usually, the gait period was classified based on the GRF because it is based on heel-contact, heel-off, and toe-off. We wanted to ensure that the identification of the gait period was possible without the GRF signal. Therefore, the gait period was distinguished using a combination of sensors. Fig. 6 shows the results of the gait period classification into seven (loading response, mid-stance, terminal stance, pre-swing, initial swing, mid-swing, and terminal swing) and six (loading response, mid-stance, terminal stance, pre-swing, initial swing, and mid-swing+ terminal swing) periods. The results of the classification into the GRF, which determines the gait period, were the most accurate in the single sensor combination. However, in the seven-gait-period classification, the accuracy was not 100% because the sum of the four GRF sensors was used to distinguish the middle and terminal swings because different averages for each sensor were used as features. Fig. 6 shows that gait period classification with sEMG is more accurate than with a single sensor. When used with sEMG together, the performance of GRF increased by 0.5%, the position increased by 1.7%, and the interaction force increased by 65.5% in the seven-gait-period classification. Very low classification accuracy was

shown when using only the interaction force, which implies that the interaction force sensor does not make a significant difference in the classification of the gait periods. The low association with the gait period of IntF made the result of the combination of IntF and EMG the same as that obtained using EMG alone. This shows that IntF is an effective variable in walking environment classification but has no meaning in gait period classification.

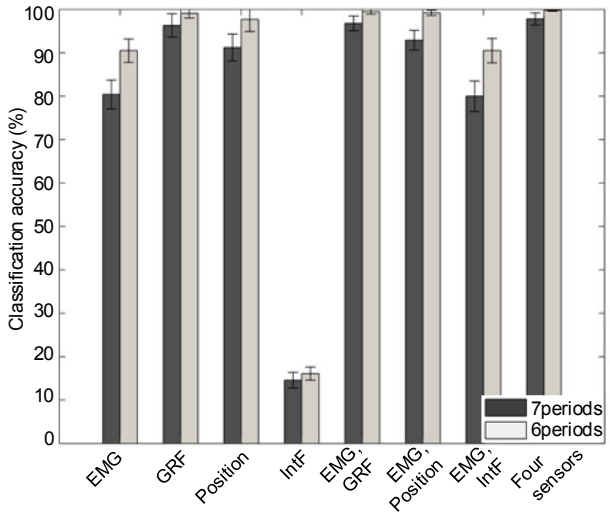


**Fig. 6 Gait period classification results in seven and six periods according to sensor combinations**

In the six-gait-period classification, the GRF reference classification accuracy was close to 100% because it was the gait period classification that combined mid-swing and terminal swing. Additionally, when two sensor combinations were used, the "EMG, GRF" combination had better performance. With the exception of the GRF sensor, the classification accuracy of the "EMG, Position" combination was high.

### 3.2.2 Combination of sEMG sensor locations

In the classification of the gait periods, the accuracy using combinations of sEMG sensor positions with the GRF, position, and interaction force sensors was also not significantly different among the subjects shown in Section 3.1.2. Therefore, we analyzed sEMG position combinations suitable for the classification of gait periods using only the sEMG sensors. Table 5 shows the gait period classification performance according to sEMG sensor locations. The sEMG sensor for all the positions and the sEMG sensor for the four muscles around the knee differed by 3%. Unlike environment classification, the accuracy of the two-position sEMG sensor was less than 10% of the accuracy of the sEMG sensor for all positions. Similar to environment classification, the accuracy of the combination of VM and GAS was the highest in the two sensor positions. Therefore, the most effective muscles in the environment and gait period classification are VM and GAS.

**Table 5 Gait period classification results according to the combinations of sEMG sensor locations without other sensors**

| Sensor combination | Classification accuracy (%) |
|---|---|
| All locations | 80.4±3.3 |
| VM, HAM, TA, GAS | 77.7±4.9 |
| VM, TA | 61.3±4.7 |
| VM, GAS | 68.0±7.7 |
| HAM, GAS | 67.9±7.8 |
| TA, GAS | 67.1±9.0 |

### 3.2.3 Combination of sEMG sensor features

We compared the effective combinations of sEMG features in gait period detection. Similar to the above results, the inclusion of the other sensors was not effective and thus was not compared. The effect of the combination of the sEMG features was compared using only the sEMG sensor. Fig. 7 shows the gait period classification performance according to sEMG feature combinations. For a single feature, the ZC result was the highest, 70.9%. When using SSC as a

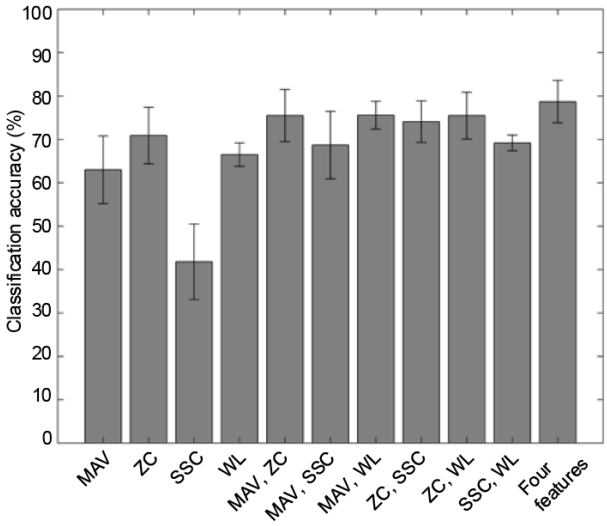


**Fig. 7 Gait period classification results according to the sEMG feature combinations without other sensors**

single feature, the accuracy was less than 50%, as in environment classification. As for two-feature combinations, the classification accuracy of "MAV, ZC", "MAV, WL," and "ZC, WL" was all 75%. When using all four sEMG features, the classification accuracy was 78%. The combination of "MAV, ZC" or "MAV, WL" was the most appropriate for both cases when compared to the results of environment classification.

## 4 Conclusions

In this study, sEMG signals were used together with various sensors to identify the gait period and walking environment. Four people performed a walking test in five different environments: level walking, ramp ascent/descent, and stair ascent/descent. To achieve effective data sensing, data design was performed under various conditions. We classified the walking environment and gait period by a combination of sEMG, GRF, position, and interaction force sensors. When using only the sEMG sensor, effective combinations were found for each sEMG sensor location and sEMG feature.

As for sensor combinations, the classification performances of the GRF sensor and interaction force sensor were increased by 7% to 10%, when classified together with the sEMG sensor in environment classification. In gait period classification, when the interaction force sensor was classified with the sEMG sensor, the performance increased by 65% to 75%. Additionally, when using the remaining three sensors without the GRF sensor, the environment classification accuracy was 96.0% for preHC and 94.1% for preTO. The gait period classification result was 92.6% in the seven gait periods, and 99.2% in the six gait periods. For the position of the sEMG sensor, the VM and GAS muscle combination was the most accurate when choosing two of the five lower limb muscles. In this case, only the sEMG sensor was used. The performance of environment classification was 74.4% for preHC and 71.7% for preTO, and the gait period classification result was 68.0%. These results were 2.2%, 6.1%, and 12.3% lower than the result when using all five muscles, respectively. The combination of "MAV, ZC" or "MAV, WL" was the effective combination of the two sEMG features. In the case of the "MAV, ZC" combination, the environment classification had an accuracy of 80.0% for preHC and 77.1% for preTO, and the gait period classification had an accuracy of 75.5%. This result is 3.3% higher in the preHC case, 0.6% lower in the preTO case, and 3.2% lower in gait period classification than in the case of using the sEMG features, MAV, ZC, SSC, and WL.

The purpose of this study is to show progress with the use of sEMG when recognizing a walking environment and gait period with other sensors. In conclusion, using sEMG resulted in a higher accuracy compared to using only mechanical sensors. Therefore, using sEMG signals can enhance understanding of walking intention. When the sEMG is used, the VM and GAS muscle combination is recommended for the position of the sEMG sensor, and "MAV, ZC" or "MAV, WL" combination is recommended for the sEMG features.

## References

Cifrek M, Medved V, Tonković S, et al., 2009. Surface EMG based muscle fatigue evaluation in biomechanics. *Clin Biomech*, 24(4):327-340. https://doi.org/10.1016/j.clinbiomech.2009.01.010

Colombo G, Joerg M, Schreier R, et al., 2000. Treadmill training of paraplegic patients using a robotic orthosis. *J Rehabil Res Dev*, 37(6):693-700.

Dotov DG, Bardy BG, Dalla Bella S, 2016. The role of environmental constraints in walking: effects of steering and sharp turns on gait dynamics. *Sci Rep*, 6:28374. https://doi.org/10.1038/srep28374

Du L, Zhang F, Liu M, et al., 2012. Toward design of an environment-aware adaptive locomotion-mode-recognition system. *IEEE Trans Biomed Eng*, 59(10): 2716-2725. https://doi.org/10.1109/TBME.2012.2208641

Esquenazi A, Talaty M, Packel A, et al., 2012. The rewalk powered exoskeleton to restore ambulatory function to individuals with thoracic-level motor-complete spinal cord injury. *Am J Phys Med Rehabil*, 91(11):911-921. https://doi.org/10.1097/PHM.0b013e318269d9a3

Farrell MT, 2013. Pattern Classification of Terrain during Amputee Walking. PhD Thesis, Massachusetts Institute of Technology, Massachusetts, USA.

Goršič M, Kamnik R, Ambrožič L, et al., 2014. Online phase detection using wearable sensors for walking with a robotic prosthesis. *Sensors*, 14(2):2776-2794. https://doi.org/10.3390/s140202776

Guizzo E, Goldstein H, 2005. The rise of the body bots [robotic exoskeletons]. *IEEE Spectr*, 42(10):50-56. https://doi.org/10.1109/MSPEC.2005.1515961

Gupta R, Agarwal R, 2018. Continuous human locomotion identification for lower limb prosthesis control. *CSI Trans ICT*, 6(1):17-31. https://doi.org/10.1007/s40012-017-0178-4

Huang H, Kuiken TA, Lipschutz RD, 2009. A strategy for identifying locomotion modes using surface electromyo-

graphy. *IEEE Trans Biomed Eng*, 56(1):65-73. https://doi.org/10.1109/TBME.2008.2003293

Huang H, Zhang F, Hargrove LJ, et al., 2011. Continuous locomotion-mode identification for prosthetic legs based on neuromuscular–mechanical fusion. *IEEE Trans Biomed Eng*, 58(10):2867-2875. https://doi.org/10.1109/TBME.2011.2161671

Jin DW, Yang JK, Zhang RH, et al., 2006. Terrain identification for prosthetic knees based on electromyographic signal features. *Tsinghua Sci Technol*, 11(1): 74-79. https://doi.org/10.1016/S1007-0214(06)70157-2

Jung JY, Heo W, Yang H, et al., 2015. A neural network-based gait phase classification method using sensors equipped on lower limb exoskeleton robots. *Sensors*, 15(11): 27738-27759. https://doi.org/10.3390/s151127738

Kawamoto H, Lee S, Kanbe S, et al., 2003. Power assist method for HAL-3 using EMG-based feedback controller. Proc IEEE Int Conf on Systems, Man and Cybernetics, p.1648-1653. https://doi.org/10.1109/ICSMC.2003.1244649

Kim H, Shin YJ, Kim J, 2017a. Kinematic-based locomotion mode recognition for power augmentation exoskeleton. *Int J Adv Rob Syst*, 14(5):1-14. https://doi.org/10.1177/1729881417730321

Kim H, Shin YJ, Kim J, 2017b. Design and locomotion control of a hydraulic lower extremity exoskeleton for mobility augmentation. *Mechatronics*, 46:32-45. https://doi.org/10.1016/j.mechatronics.2017.06.009

Kong K, Tomizuka M, 2009. A gait monitoring system based on air pressure sensors embedded in a shoe. *IEEE/ASME Trans Mechatron*, 14(3):358-370. https://doi.org/10.1109/TMECH.2008.2008803

Lawson BE, Varol HA, Huff A, et al., 2013. Control of stair ascent and descent with a powered transfemoral prosthesis. *IEEE Trans Neur Syst Rehabil Eng*, 21(3): 466-473. https://doi.org/10.1109/TNSRE.2012.2225640

Lenzi T, de Rossi SMM, Vitiello N, et al., 2012. Intention-based EMG control for powered exoskeletons. *IEEE Trans Biomed Eng*, 59(8):2180-2190. https://doi.org/10.1109/TBME.2012.2198821

Lenzi T, Carrozza MC, Agrawal SK, 2013. Powered hip exoskeletons can reduce the user's hip and ankle muscle activations during walking. *IEEE Trans Neur Syst Rehabil Eng*, 21(6):938-948. https://doi.org/10.1109/TNSRE.2013.2248749

Lewis CL, Ferris DP, 2011. Invariant hip moment pattern while walking with a robotic hip exoskeleton. *J Biomech*, 44(5):789-793. https://doi.org/10.1016/j.jbiomech.2011.01.030

Long Y, Du ZJ, Wang WD, et al., 2016. PSO-SVM-based online locomotion mode identification for rehabilitation robotic exoskeletons. *Sensors*, 16(9):1-20. https://doi.org/10.3390/s16091408

Martinez-Hernandez U, Rubio-Solis A, Dehghani-Sanij AA, 2018. Recognition of walking activity and prediction of gait periods with a CNN and first-order MC strategy. 7th IEEE Int Conf on Biomedical Robotics and Biomechatronics, p.897-902. https://doi.org/10.1109/BIOROB.2018.8487220

Neumann DA, 2002. Kinesiology of the Musculoskeletal System: Foundations for Rehabilitation. Mosby, Inc., St. Louis, USA.

Perry J, Davids JR, 1992. Gait analysis: normal and pathological function. *J Pediatr Orthop*, 12(6):815.

Sankai Y, 2010. HAL: hybrid assistive limb based on cybernics. In: Kaneko M, Nakamura Y (Eds.), Robotics Research. Springer Berlin Heidelberg, p.25-34. https://doi.org/10.1007/978-3-642-14743-2_3

Sanz-Merodio D, Cestari M, Arevalo JC, et al., 2014. Generation and control of adaptive gaits in lower-limb exoskeletons for motion assistance. *Adv Robot*, 28(5): 329-338. https://doi.org/10.1080/01691864.2013.867284

Sasaki D, Noritsugu T, Takaiwa M, 2013. Development of pneumatic lower limb power assist wear driven with wearable air supply system. IEEE/RSJ Int Conf on Intelligent Robots and Systems, p.4440-4445. https://doi.org/10.1109/IROS.2013.6696994

Strausser KA, Kazerooni H, 2011. The development and testing of a human machine interface for a mobile medical exoskeleton. IEEE/RSJ Int Conf on Intelligent Robots and Systems, p.4911-4916. https://doi.org/10.1109/IROS.2011.6095025

Varol HA, Sup F, Goldfarb M, 2010. Multiclass real-time intent recognition of a powered lower limb prosthesis. *IEEE Trans Biomed Eng*, 57(3):542-551. https://doi.org/10.1109/TBME.2009.2034734

Veneman JF, Kruidhof R, Hekman EEG, et al., 2007. Design and evaluation of the lopes exoskeleton robot for interactive gait rehabilitation. *IEEE Trans Neur Syst Rehabil Eng*, 15(3):379-386. https://doi.org/10.1109/TNSRE.2007.903919

Walsh CJ, Endo K, Herr H, 2007. A quasi-passive leg exoskeleton for load-carrying augmentation. *Int J Hum Robot*, 4(3):487-506. https://doi.org/10.1142/S0219843607001126

Yan TF, Cempini M, Oddo CM, et al., 2015. Review of assistive strategies in powered lower-limb orthoses and exoskeletons. *Robot Auton Syst*, 64:120-136. https://doi.org/10.1016/j.robot.2014.09.032

Young AJ, Ferris DP, 2017. State of the art and future directions for lower limb robotic exoskeletons. *IEEE Trans Neur Syst Rehabil Eng*, 25(2):171-182. https://doi.org/10.1109/TNSRE.2016.2521160

Young AJ, Simon A, Hargrove LJ, 2013. An intent recognition strategy for transfemoral amputee ambulation across different locomotion modes. 35th Annual Int Conf IEEE Engineering in Medicine and Biology Society, p.1587-1590. https://doi.org/10.1109/EMBC.2013.6609818

Young AJ, Kuiken TA, Hargrove LJ, 2014. Analysis of using EMG and mechanical sensors to enhance intent recognition in powered lower limb prostheses. *J Neur Eng*, 11(5):056021. https://doi.org/10.1088/1741-2560/11/5/056021

Zhang F, Fang Z, Liu M, et al, 2011. Preliminary design of a terrain recognition system. Annual Int Conf IEEE Engineering in Medicine and Biology Society, p.5452-5455. https://doi.org/10.1109/IEMBS.2011.6091391

Zoss AB, Kazerooni H, Chu A, 2006. Biomechanical design of the Berkeley lower extremity exoskeleton (bleex). *IEEE/ASME Trans Mechatron*, 11(2):128-138. https://doi.org/10.1109/TMECH.2006.871087